


Momentum-dependent electron-phonon coupling in charge density wave systems

Jean-Paul Pouget 

Laboratoire de Physique des Solides, CNRS UMR 8502, Université de Paris-Sud, Université Paris-Saclay, 91405 Orsay, France

Enric Canadell 

Institut de Ciència de Materials de Barcelona, ICMAB-CSIC, Campus Bellaterra, 08193 Barcelona, Spain

Bogdan Guster 

Institute of Condensed Matter and Nanosciences, Université Catholique de Louvain, Chemin des étoiles 8, B-1348 Louvain-la-Neuve, Belgium



(Received 16 December 2020; revised 24 February 2021; accepted 5 March 2021; published 18 March 2021)

Many charge density wave (CDW) systems exhibit $q(T)$ electron-hole modulations continuously varying with T and saturating upon cooling at an incommensurate value even if the maximum occurring in the electron-hole Lindhard response does not exhibit such a thermal shift. Using a simple RPA argument we show that the experimental $q(T)$ can be understood if the electron-phonon coupling (EPC) $g(q)$, necessary to set coupled electronic and structural modulations, is momentum dependent. In this analysis, the sense of variation of $q(T)$ depends upon the sign of $\frac{\partial g(q)}{\partial q}$ and its amplitude of thermal variation is controlled by the electron-hole coherence length (or CDW rigidity) in the modulation direction. This model quantitatively accounts for the thermal dependence of $q(T)$ in the one-dimensional (1D) CDW system $K_{0.3}MoO_3$ (blue bronze) both in its CDW ground state and in its pretransitional CDW fluctuation regime. We suggest that such a general analysis can be extended to account for the $q(T)$ dependence observed in other 1D and 2D CDW systems such as the transition metal di- and trichalcogenides as well as the lanthanide and rare-earth tritellurides. Using a detailed analysis of the low frequency phonon spectrum of the blue bronze, we then propose a new scenario for the q dependent EPC, where $g(q)$ is due to a momentum-dependent hybridization between the critical phonon branch bearing the Kohn anomaly and other low-lying phonon branches. This allows obtaining a sign of $\frac{\partial g(q)}{\partial q}$ in agreement with that deduced from the analysis of $q(T)$. Finally, we propose that similar hybridization effects could also be relevant for other 1D and 2D CDW systems exhibiting a thermally dependent modulation.

DOI: [10.1103/PhysRevB.103.115135](https://doi.org/10.1103/PhysRevB.103.115135)

I. INTRODUCTION

Many low-dimensional metals undergo electron-hole or density wave instabilities associated with an anisotropic band structure which often coexists with electron-electron or Cooper pairing interactions. This generally leads to complex phase diagrams exhibiting intertwined orders where in many cases spin or charge density wave (SDW or CDW) modulation coexists or competes with superconductivity [1]. Typical examples can be found among the cuprates [2], transition metal dichalcogenides [3], and organic conductors [4]. In low-dimensional metals, the momentum-dependent q maximum of the electron-hole response (below referred to as Lindhard function for noninteracting electrons) arises from the nesting of a large portion of electronic states located at each side of the Fermi level [1]. This is typically the case of one-dimensional (1D) electronic systems where the Lindhard function exhibits a maxima for $q = 2k_F$ which diverges upon cooling (k_F is the Fermi wave vector of the 1D band structure) [5]. When the electron gas is coupled to a phonon branch through the electron-phonon coupling (EPC), the electron-hole instability drives a Peierls transition below T_{CDW} stabilizing a CDW modulation together with a periodic lattice distortion (PLD) in

quadrature with the CDW [6]. This $2k_F$ weak coupling Peierls scenario is well documented from *ab initio* calculations of the Lindhard function in 1D conductors such as the blue bronze $K_{0.3}MoO_3$ [7] and the transition metal trichalcogenide $NbSe_3$ [8]. However, such a scenario is not clearly established for two-dimensional (2D) electronic systems like $2H-NbSe_2$ and $CeTe_3$ because their Lindhard response does not exhibit clear-cut q maxima [9]. Thus, more elaborate microscopic approaches taking into account explicitly the wave vector dependence of the EPC $g(k, q)$ [10,11] have been recently developed for the case of the transition metal dichalcogenides [12–15]. Scenarios where the CDW modulation is mainly selected by the sizably q dependent EPC have also been proposed [16–18].

A related phenomena, which has not yet received a suitable explanation, is that in many cases the CDW modulation wave vector $q(T)$ is found to vary with temperature between T_{CDW} and 0 K by a few percent. Table I reports selected examples of 1D and 2D CDW systems where $q(T)$ varies upon cooling below T_{CDW} with a phenomenological thermally activated law

$$\delta q(T) = q(T) - 2k_F \propto e^{-\frac{\Delta_{\text{eff}}}{k_B T}}, \quad (1)$$

TABLE I. Selected 1D and 2D metals presenting a CDW ground state with a continuous thermal variation of $q(T)$ below T_{CDW} . The 0 K modulation wave vector $2k_F$ is indicated together with the relative variation $\frac{\delta q(T)}{2k_F}$ between 0 K and T_{CDW} . The effective energy Δ_{eff} defined by Eq. (1), and determined from experimental data with an accuracy of 10%, is also given. In the blue bronze $\text{K}_{0.3}\text{MoO}_3$ the deviation ϵ at $0.75b^*$ which ranges from 5×10^{-4} to 40×10^{-4} in the literature [19] is ascribed to sample nonstoichiometry.

Compound	T_{CDW}	$2k_F$ (0 K)	$\frac{\delta q(T)}{2k_F}$ in [0 K, T_{CDW}]	Δ_{eff} (K)	Ref.
$\text{K}_{0.3}\text{MoO}_3$	180 K	$(0.75-\epsilon)b^*$	-1.54%	525	[19]
NbSe_3	144 K	$0.241b^*$	+1.5%	550	[26]
$2H\text{-NbSe}_2$	33.5 K	$0.327a^*$	-1.5%	~ 100	[23,27]
TbTe_3	333 K	$0.291c^*$	+2.1%	500	[28]

which involves an effective energy Δ_{eff} . In the compounds of this table the modulation saturates at 0 K at an incommensurate $q(0)$ value [$2k_F$ in Eq. (1)], and the continuous variation of $q(T)$ does not exhibit any evidence of lock-in transition at a commensurate value. A typical $q(T)$ variation is shown in Fig. 1 for $\text{K}_{0.3}\text{MoO}_3$ [19]. Note that similar activated thermal dependencies are also observed in three-dimensional (3D) metallic CDW systems such as $\alpha\text{-U}$ [20]. This thermally activated wave vector dependence is observed both for $\delta q(T)$ in sinusoidal CDW systems ($\text{K}_{0.3}\text{MoO}_3$, NbSe_3) and for the $n\delta q(T)$ harmonics in nonsinusoidal CDW systems ($\alpha\text{-U}$, $2H\text{-NbSe}_2$, TbTe_3). Since the same behavior is observed regardless of the shape of the modulation, $\delta q(T)$ does not originate from the development of harmonics of modulation or nucleation of discommensurations separating commensurate

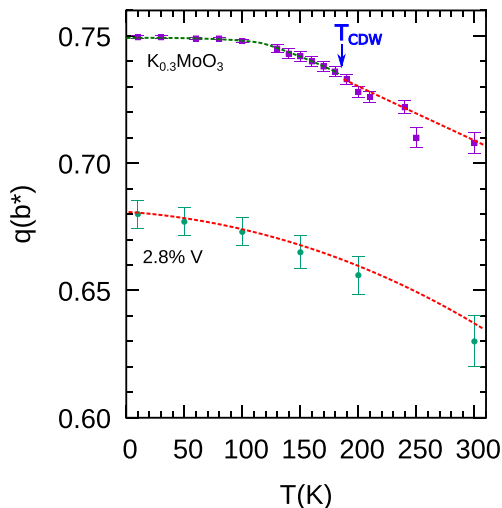


FIG. 1. Thermal dependence of the experimental CDW modulation wave vector $q(T)$ in the b chain direction of $\text{K}_{0.3}\text{MoO}_3$ and the alloy $\text{K}_{0.3}\text{Mo}_{1-x}\text{V}_x\text{O}_3$ with $x = 2.8\%$. The continuous lines are fits of $\delta q(T)$ below T_{CDW} for $\text{K}_{0.3}\text{MoO}_3$ using $\xi_{\text{eh}}^{\text{SC}}(T)$ given by Eq. (15) (blue line) and above T_{CDW} of $\text{K}_{0.3}\text{MoO}_3$ as well as for $\text{K}_{0.3}\text{Mo}_{1-x}\text{V}_x\text{O}_3$ at any T , using $\xi_{\text{eh}}^{\text{M}}(T)$ taken from Eq. (9) or Ref. [7] (red lines). In the blue bronze data shown here, $q(0) = 0.7495(5)b^*$ [19]. The experimental data are taken from [22].

domains [21]. In 1D CDW systems this dependence is not due to the electron-hole response itself because, as recently verified for $\text{K}_{0.3}\text{MoO}_3$ [7] and NbSe_3 [8], the maxima of the Lindhard response does not vary appreciably with temperature.

An important observation is that the thermal variation $\delta q(T)$ of the critical wave vector of quasi-1D pretransitional CDW fluctuations, measured above T_{CDW} in the metallic phase of the blue bronze, varies in continuity with $\delta q(T)$ measured below T_{CDW} [19] (Fig. 1). A $\delta q(T)$ of the same magnitude is also measured for residual quasi-1D CDW fluctuations in the disordered blue bronze when a large amount of V, which substitutes Mo, is able to suppress the Peierls transition [22] (Fig. 1). These facts mean that the thermal dependence of $\delta q(T)$ should be related to the intrachain mechanism of the Peierls instability and that the interchain coupling plays a minor role. Therefore it is difficult to rationalize these data on the basis of the recent proposal that $\delta q(T)$ is controlled by the thermal dependence of the 3D CDW order parameter [23].

All these features mean that, beyond specific microscopic models, there is a quite general mechanism governing the thermal dependence of the CDW modulation wave vector $q(T)$. Below, using a simple RPA mechanism of the Peierls transition, we propose that the thermal shift of the modulation momentum $\delta q(T)$ is caused by a q dependent EPC $g(q)$, where the k dependence of $g(k, q)$ has been neglected. To provide support for this statement we calculate the thermal variation of $\delta q(T)$ above and below T_{CDW} for the blue bronze. Our calculation shows that the thermal dependence of $\delta q(T)$ is controlled by the rigidity of the CDW sublattice, defined as its response to a momentum variation via the thermal dependence of the electron-hole coherence length $\xi_{\text{eh}}(T)$. This allows obtaining the magnitude and sense of variation of the momentum dependence of the EPC $|g(q)|$. A long time ago it was shown [24] that the momentum dependence of the EPC in transition metals has an electronic origin and recent works [12–15] have extended this idea for transition metal dichalcogenides. Below we propose an additional mechanism of the momentum dependence of the EPC. More precisely we propose that $g(q)$ can be due to hybridization of low-lying phonon branches of the same symmetry near $2k_F$, including the critical phonon mode responsible of the PLD below T_{CDW} and which presents a stronger EPC with the low-dimensional electron gas than the other phonon branches.

II. RESULTS AND DISCUSSION

A. Thermal dependence of the modulation wave vector

1. In the metallic state

In this section we use the simplest formalism developed to analyze the Peierls transition in 1D conductors [5] as well as to treat the density wave instabilities in conductors of higher dimension [25]. We neglect electron-electron effects which apparently do not play a dominant role in the physics of low-dimensional metals like transition metal bronzes and chalcogenides which do not exhibit magnetism and Mott-Hubbard localization effects. We thus consider that the dominant interaction driving a $2k_F$ -like CDW ground state

is the EPC. The EPC theory in metals explicitly derives a momentum-dependent coupling $g(k, q)$ [11]. This wave vector dependence is often neglected for simplicity in earlier theories developing the CDW instability. However, there are still unexplained experimental facts such as the thermal variation of the CDW modulation wave vector considered in this section, which clearly prove that the assumption of a nonmomentum variation of the EPC should be revised.

According to the RPA approximation, the CDW instability in the metallic state is driven by the divergence of the response function

$$\chi_{\text{CDW}}(q) = \frac{\chi_{\text{eh}}(q)}{1 - D_2(q)}, \quad (2)$$

where $D_2(q)$ is the structured electronic susceptibility including the momentum-dependent EPC $g(k, q)$ [29],

$$D_2(q) = \frac{1}{\hbar\Omega_0(q)} \sum_k |g(k, q)|^2 \frac{f(\epsilon_k) - f(\epsilon_{k+q})}{\epsilon_{k+q} - \epsilon_k}. \quad (3)$$

If the k dependence of the EPC is neglected [30], then

$$D_2(q) \approx \lambda(q)\chi_{\text{eh}}(q), \quad (4)$$

where $\chi_{\text{eh}}(q)$ is the Lindhard response and $\lambda(q)$ is the q dependent reduced EPC:

$$\lambda(q) = \frac{|g(q)|^2}{\hbar\Omega_0(q)}. \quad (5)$$

In Eq. (5) $|g(q)|$ is the modulus of the EPC and $\Omega_0(q)$ is the bare frequency of the critical phonon mode which drives the PLD. The wave vector of the modulation is given by minimization of the denominator in Eq. (2) where $D_2(q)$ is approximated by Eq. (4) or maximization of the product $\lambda(q)\chi_{\text{eh}}(q)$:

$$\frac{\partial \ln \lambda(q)}{\partial q} + \frac{\partial \ln \chi_{\text{eh}}(q)}{\partial q} = 0. \quad (6)$$

In the metallic state of the Peierls chain, $\chi_{\text{eh}}(q)$ has a maximum at $2k_F$ and a Lorentzian shape for $\delta q = q - 2k_F$:

$$\chi_{\text{eh}}(q) = \frac{\chi_{\text{eh}}(2k_F)}{1 + (\delta q \xi_{\text{eh}})^2}. \quad (7)$$

From Eq. (7) it can be deduced at first order in δq that if $\lambda(q)$ depends of q , then q shifts from $2k_F$ by

$$\frac{\delta q(T)}{2k_F} = k_F \frac{\partial \ln \lambda(q)}{\partial q} \frac{1}{[2k_F \xi_{\text{eh}}(T)]^2}. \quad (8)$$

The sign of $\frac{\delta q(T)}{2k_F}$ is that of the logarithmic derivative $\frac{\partial \ln \lambda(q)}{\partial q}$, and the thermal dependence of $\delta q(T)$ is governed by the inverse square of the electron-hole coherence length $\xi_{\text{eh}}(T)$.

In the 1D fluctuation regime of the Peierls chain above T_{CDW} one simply has [31]

$$\xi_{\text{eh}}^M(T) = \frac{\sqrt{7\zeta(3)}\hbar v_F}{4\pi k_B T}, \quad (9)$$

where v_F is the Fermi velocity. In real materials $\xi_{\text{eh}}^M(T)$ can be directly obtained from the inverse half-width at half-maximum (HWHM) of the Lorentzian shape in the chain direction of the *ab initio* Lindhard function [Eq. (7)] [7,8].

TABLE II. $k_F \frac{\partial \ln \lambda(q)}{\partial q}$ in selected CDW systems deduced [Eq. (8)] from calculated or experimentally determined $[\xi_{\text{eh}}(T)]^{-1}$ and the experimental $\delta q(T)/2k_F$. $k_F \frac{\partial \ln \lambda(q)}{\partial q}$ is given with an error bar estimated from the uncertainties on the determination of $q(T)$ and $[\xi_{\text{eh}}(T)]^{-1}$.

Compound	T	$[\xi_{\text{eh}}(T)]^{-1}$	$k_F \frac{\partial \ln \lambda(q)}{\partial q}$	Ref.
$\text{K}_{0.3}\text{MoO}_3$	$T > T_{\text{CDW}}$	HWHM of $\chi_{\text{eh}}(q)$	-8.1 ± 1.6	[7]
$\text{K}_{0.3}\text{MoO}_3$	$T < T_{\text{CDW}}$	Eq. (15)	-9.5 ± 1.4	-
$\text{K}_{0.3}\text{Mo}_{1-x}\text{V}_x\text{O}_3$	$T < 300$ K	HWHM of $\chi_{\text{eh}}(q)$	-7.8 ± 1.6	-
$x = 2.8\%$				
NbSe_3	T_{CDW}	$0.024b^*$ [HWHM of $\chi_{\text{eh}}(q)$]	$+4 \pm 1.4$	[8]
$2H\text{-NbSe}_2$	T_{CDW}	$0.046a^*$ (HWHM of the squared Kohn anomaly [Eq. (10)])	-0.8 ± 0.24	[16]
TbTe_3	T_{CDW}	$0.030c^*$ (HWHM of the squared Kohn anomaly [Eq. (10)])	$+2.0 \pm 0.8$	[17]

$\xi_{\text{eh}}^M(T)$ can be also extracted from the curvature of the Kohn anomaly experimentally measured near $2k_F$ and given by

$$(\xi_{\text{eh}}^M)^2 = \frac{1}{(\Omega_0^2 - \Omega_{2k_F}^2)} \frac{\partial \Omega_q^2}{\partial q^2}, \quad (10)$$

where Ω_q is the q dependent Kohn anomaly whose minimum occurs at $q = 2k_F$, and Ω_0 is the frequency of the bare phonon mode bearing the Kohn anomaly. Here $\xi_{\text{eh}}^M(T)$ is obtained according to Eq. (10) from the HWHM of the squared frequency of the Kohn anomaly.

In the 1D compounds $\text{K}_{0.3}\text{MoO}_3$ and NbSe_3 , where the total Lindhard response is a sum of individual Lorentzians [7,8], the $\xi_{\text{eh}}^M(T)$ considered in Table II is obtained from the inverse HWHM of the $2k_F$ response. This procedure cannot be applied for 2D materials such as $2H\text{-NbSe}_2$ and the lanthanide and rare-earth tellurides because the calculated Lindhard function is broad and not really peaked at the critical CDW wave vector [9,32]. This is due to the absence of important nesting effects for a large portion of electronic states. However, recent calculations [12,13] using a model band structure for $2H\text{-NbSe}_2$ have shown that, due to the momentum-dependent EPC $g(k, q)$, a peak occurs in $D_2(q)$ at the CDW modulation wave vector. This model thus leads to the formation of a well defined Kohn anomaly at this wave vector in agreement with experimental measurements. In addition, it predicts the thermal variation of the CDW wave vector in the related VSe_2 compound [14]. Thus, in the case of dichalcogenides and tritellurides we will use the $\xi_{\text{eh}}^M(T)$ values (Table II) obtained with Eq. (10) from the curvature of the Kohn anomaly experimentally measured for $2H\text{-NbSe}_2$ [16] and TbTe_3 [17]. Note that in the case of the blue bronze, $\xi_{\text{eh}}^M(T)$ deduced from the curvature of the Kohn anomaly consistently amounts to $\xi_{\text{eh}}^M(T)$ deduced from the inverse HWHM of the Lorentzian shaped Lindhard function [7].

Equation (9) inserted into Eq. (8) leads to a T^2 dependence of $\frac{\delta q(T)}{2k_F}$. Such a thermal dependence is quantitatively observed over a large T range for the CDW modulation wave vector of

the 2.8% V substituted blue bronze which does not exhibit a long range CDW order [22] (Fig. 1). Taking $\xi_{\text{ch}}^M(T)$ from the inverse HWHM of the Lorentzian profile of the *ab initio* electron-hole response of the blue bronze [7], the best fit of $\frac{\delta q(T)}{2k_F}$ leads to $k_F \frac{\partial \ln \lambda(q)}{\partial q} \approx -8.1$ and -7.8 for the pristine blue bronze above T_{CDW} and the 2.8% V substituted blue bronze for the whole T range, respectively (Table II).

For a CDW system where $\lambda(q)$ is given by Eq. (5) it follows that the CDW critical wave vector is defined by

$$k_F \frac{\partial \ln \lambda(q)}{\partial q} = 2k_F \frac{\partial \ln |g(q)|}{\partial q} - k_F \frac{\partial \ln \Omega_0(q)}{\partial q}. \quad (11)$$

With a q dependent bare frequency of the phonon branch bearing the Kohn anomaly in the blue bronze [7] of $\frac{\Omega_0(2k_F)k_F}{\Omega_0(2k_F)} = +0.46$, one obtains $2k_F \frac{\partial \ln |g(q)|}{\partial q} \approx -7.6$ for the momentum-dependent reduced EPC in the metallic state. $k_F \frac{\partial \ln \lambda(q)}{\partial q}$ cannot be determined in the metallic phase of other CDW compounds considered in Table I because no measurements of $\delta q(T)$ have been performed above T_{CDW} .

2. In the Peierls ground state

In the semiconducting ground state of the Peierls chain with a thermally dependent gap Δ , the q dependent free energy is the sum of a 1D electronic part and the energy cost for setting the CDW modulation [31]

$$F(q) = \int_0^\Delta \Delta' \chi_{\text{eh}}(q, \Delta') d\Delta' + \frac{N(E_F)\Delta^2}{\lambda(q)}. \quad (12)$$

The electronic free energy minimum for $q = 2k_F$ is expressed as $F_{\text{el}}(2k_F) = -N(E_F)\Delta^2$ where $N(E_F)$ is the density of states at the Fermi level of the metallic state. At the lowest order in δq , the electronic part of the free energy can be developed as [31]

$$F_{\text{el}}(q) \approx F_{\text{el}}(2k_F)[1 - (\delta q \xi_{\text{ch}}^{\text{SC}})^2], \quad (13)$$

where $\xi_{\text{ch}}^{\text{SC}}$, the electron-hole coherence length in the Peierls ground state, quantifies the rigidity of the CDW lattice with respect to a variation of its modulation wave vector. The modulation wave vector is thus fixed by the minimum of the product $\lambda(q)F_{\text{el}}(q)$ and consequently, Eq. (8) is recovered.

The calculation of $\xi_{\text{ch}}^{\text{SC}}$ is quite tedious. For a simple Peierls chain with a full gap opening (Δ), it can be shown that within the mean-field approximation, in the low temperature limit $k_B T \ll \Delta/2$ [31,33],

$$\xi_{\text{ch}}^{\text{SC}}(T) = 2\hbar v_F \sqrt{\frac{k_B T}{\pi \Delta^3}} e^{\frac{\Delta}{2k_B T}}. \quad (14)$$

Equation (14) shows that the electron-hole coherence length (CDW rigidity) increases exponentially upon cooling. This feature qualitatively accounts for the exponential decrease of $\delta q(T)$ for the compounds quoted in Table I. Note however that the Peierls gap Δ entering in Eq. (14) depends upon the temperature as it does the order parameter η of the Peierls transition ($\Delta = \eta \Delta_0$). Note also that the prefactor of the exponential varies with T . Both effects explain why Δ_{eff} in Table I is only a fraction of the 0 K Peierls gap Δ_0 .

From Eq. (14) one can also write $(2k_F \xi_{\text{ch}}^{\text{SC}})^{-1}$ as [31]

$$(2k_F \xi_{\text{ch}}^{\text{SC}})^{-1} \approx \frac{\Delta^2}{8k_B T E_F} \frac{(\Delta_0 - \Delta)}{\Delta_0} = \frac{\Delta_0^2}{4k_B T E_F} \eta^2 (1 - \eta), \quad (15)$$

where $E_F \approx \hbar v_F k_F$ has been used. When Eq. (15) is inserted into Eq. (8) a nice fit of the thermal dependence of δq of the blue bronze below $T_{\text{CDW}} = 180$ K is obtained (see Fig. 1), using a Peierls gap $\Delta_0 = 150$ meV, a Fermi energy $E_F \approx 0.65$ eV, and the thermal dependence of the order parameter $\eta(T)$ given by the square root of the relative variation of intensity of the $2k_F$ satellite reflections [34]. From this fit one deduces that $k_F \frac{\partial \ln \lambda(q)}{\partial q} \approx -9.5$, whose value is comparable to those previously obtained in the metallic phase (see Table II).

$k_F \frac{\partial \ln \lambda(q)}{\partial q}$ cannot be determined in the CDW ground state of other CDW compounds considered in Table I because below T_{CDW} an expression more elaborate than Eq. (15) should be used. In these compounds, the modulation does not open a full Peierls gap in the band structure and the materials remain (semi)metallic below T_{CDW} . Also, additional thermal excitation processes should influence the rigidity of the CDW lattice. Nevertheless, an estimation of $k_F \frac{\partial \ln \lambda(q)}{\partial q}$ can be obtained using Eq. (8) with $\frac{\delta q(T)}{2k_F}$ determined at T_{CDW} and $(\xi_{\text{ch}}^M)^{-1}$ obtained at T_{CDW} from either the HWHM of the *ab initio* $\chi_{\text{eh}}(0, 2k_F^{\text{III}}, 0)$ component of the upper Peierls transition of NbSe₃ [8] or the HWHM of the squared frequency of the Kohn anomaly in the case of $2H$ -NbSe₂ [16] and TbTe₃ [17] [see Eq. (10)]. Such estimated $(\xi_{\text{ch}}^M)^{-1}$ values are indicated in Table II.

B. The momentum-dependent EPC

From the electron-hole coherence lengths obtained in the previous section, it is possible to obtain the $k_F \frac{\partial \ln \lambda(q)}{\partial q}$ values reported in Table II. The strongest rate of variation of $\lambda(q)$ is obtained for the blue bronze, whereas those for NbSe₃ and TbTe₃ are two and four times smaller, respectively. For $2H$ -NbSe₂, $k_F \frac{\partial \ln \lambda(q)}{\partial q}$ is one order of magnitude smaller. Note that the sign of the derivative $\frac{\partial \ln \lambda(q)}{\partial q}$ is that of $\frac{\delta q(T)}{2k_F}$. As the phonon measurements show that the slope $k_F \frac{\partial \ln \Omega_0(q)}{\partial q}$ is very small in TbTe₃ and $2H$ -NbSe₂, one has $\frac{\partial \ln \lambda(q)}{\partial q} \approx 2k_F \frac{\partial \ln |g(q)|}{\partial q}$. Note that if the EPC is independent of T , $\delta q(T)$ should scale with the thermal dependence of the inverse square of the electron-hole coherence length $\xi_{\text{ch}}^{\text{SC}}(T)$.

Taking the average of $k_F \frac{\partial \ln \lambda(q)}{\partial q}$ in the metallic and semiconducting phases of the blue bronze and subtracting $k_F \frac{\partial \ln \Omega_0(q)}{\partial q}$ in Eq. (11),

$$2k_F \frac{\partial \ln |g(q)|}{\partial q} \approx -8 \quad (16)$$

is obtained. The momentum dependence of the EPC of the blue bronze can be simply obtained by integration of Eq. (16), which leads to

$$|g(q)| = |g(2k_F)| e^{\frac{-8(q-2k_F)}{2k_F}}, \quad (17)$$

where, according to the estimation of Ref. [7], $|g(2k_F)| \approx 20$ meV. Equation (17) shows that the EPC strongly varies

with q . In particular, $|g(q)|$ decreases considerably when q increases.

Our analysis is at variance with recent proposals stating that for transition metal dichalcogenides and lanthanide and rare-earth tritellurides [16–18] the wave vector dependence of the EPC $g(q)$ drives the CDW instability by exhibiting a maximum at the experimental CDW modulation momentum (note that this assumption is also considered in certain sections of Refs. [12,13]). In such a case one should have a zero rate of momentum variation of the EPC, $\frac{\partial \ln |g(q)|}{\partial q} = 0$, at the CDW modulation wave vector. Thus, according to Eq. (8) this leads to $\frac{\delta q}{2k_F} = 0$, which contradicts the experimental data (Table I). Also, we point out that the proposal of Refs. [16–18] arises from an incomplete analysis of the momentum dependence of the damping of the critical soft mode. In the RPA approximation the q dependent damping is proportional to $|g(q)|^2$ [18]. However there is no reason for this term to vary critically at T_{CDW} . Experimentally, the damping of the Kohn anomaly behaves critically at T_{CDW} , as assessed by the enhancement of its $2k_F$ peak intensity and narrowing of its linewidth [16,17,35]. Such a feature cannot be accounted for by a simple RPA analysis. The critical behavior of the Kohn anomaly damping means that the dominant contribution is due to the anharmonicity induced for example by the low frequency critical $2k_F$ CDW/PLD fluctuations. This effect, whose explanation goes beyond the RPA approximation, has been explicitly considered in the case of the Peierls chain [36].

C. Influence of the soft phonon mode hybridization in the momentum dependence of $g(q)$

The largest momentum variation of $g(q)$ found in the blue bronze together with the analysis of its low energy phonon spectrum shown in Fig. 2 [7,35], justify the proposal of a new mechanism for the momentum variation of the EPC, which is different from the purely electronic one recently suggested for the transition-metal dichalcogenides [12,13,15].

The scenario proposed for the 1D CDW blue bronze system relies on the hybridization of the soft optical (Opt.) branch polarizing longitudinally segments of four octahedra which form the repeat unit of the 1D chain running along b (for more structural details see [7]), with the acoustic branch also polarized along the direction of the four octahedra segments (LA_2 at the A point). More precisely, Fig. 2 shows that the optical mode forms along the MA reciprocal direction a valley of soft phonons whose frequency increases when reaching the A point where it hybridizes with the LA_2 acoustic branch. The $2k_F$ Kohn anomaly is located within the q range where the frequency of the Opt. branch $\Omega_0(q)$ sizably increases rendering more efficient its hybridization with the acoustic branch. It is thus easy to understand that the EPC should decrease significantly when for a q increase the hybridization of the polar Opt. branch (where the molybdenum off center displacement within the octahedra is strongly coupled with the 1D electron gas) with the LA_2 branch (of weaker EPC) is enhanced.

Generalizing such discussion, we suggest that since the phonon spectrum of other CDW systems exhibits many low frequency branches of the same symmetry, a similar hybridization mechanism could be at the origin of the

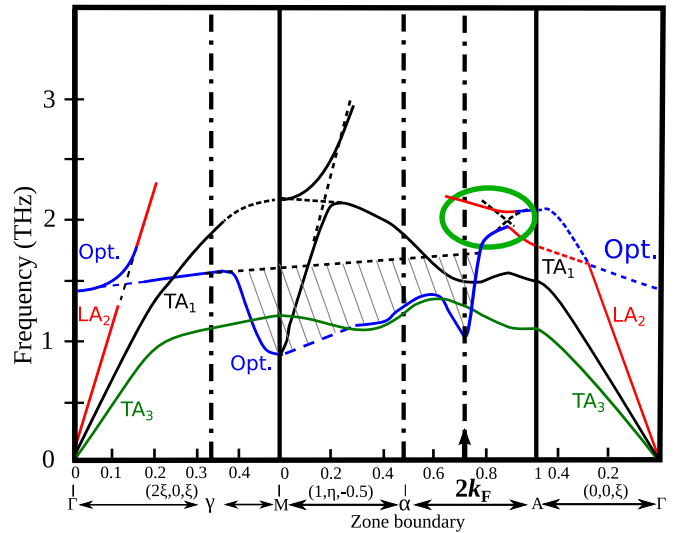


FIG. 2. Low frequency phonon branches of the blue bronze (adapted from [7]). The optical (Opt.) and acoustic (LA_2) branches which hybridize are represented in blue and red, respectively. Note the presence of a valley of soft optical phonons (hatched area). The two other low frequency acoustic branches TA_3 and TA_1 are represented in green and black, respectively. The green ellipse highlights the hybridization zone between optical and acoustic branches.

momentum variation of their EPC. Such a change, which should be corrected by the weaker variation of the phonon frequency, is approximately given by $k_F \frac{\partial \ln \lambda(q)}{\partial q}$ reported in Table II. In this scenario, the sign of the rate of variation $2k_F \frac{\partial \ln |g(q)|}{\delta q}$ (related to the variation of $\frac{\delta q}{2k_F}$) depends on the fact that the hybridization occurs for q larger than $2k_F$ [negative variation of $|g(q)|$ when q increases, as found for the blue bronze, Fig. 3(a)], or for q smaller than $2k_F$ [positive variation of $|g(q)|$ for a q increase, Fig. 3(b)].

Here we suggest that the positive variation of $\frac{\delta q}{2k_F}$ in $TbTe_3$ is due to the hybridization of the TO critical mode with low frequency optical and acoustic branches for $q < 2k_F$ [37]. We have recently found that a similar situation should occur in transition metal trichalcogenides such as TaS_3 with an

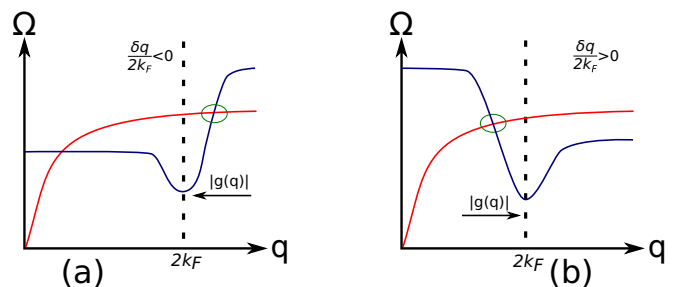


FIG. 3. Schematic representation of the hybridization (green circle) between an optical branch (in blue) strongly coupled to the electron gas, and an acoustic branch (in red) less coupled to the electron gas, which cause: (a) for $q > 2k_F$, a decrease of $|g(q)|$ when q increases, and (b) for $q < 2k_F$, an increase of $|g(q)|$ when q increases. The sign of variation of $\frac{\delta q}{2k_F}$ related to this effect is also indicated.

important hybridization between the calculated LO critical branch and transverse acoustic branches of the same symmetry for $q < 2k_F$ [8]. The origin of the weaker momentum-dependent electron-phonon coupling in $2H\text{-NbSe}_2$ could be different. In this system the critical lattice dynamics appears to be quite subtle because two low frequency longitudinal acoustic and optical phonon branches of the same Σ_1 symmetry exhibit a Kohn anomaly [38]. Also earlier phonon calculations already evidence a momentum-dependent EPC for these individual modes [39,40]. Finally, recent calculations of the shape of the Kohn anomaly in the transition metal dichalcogenides propose different mechanisms affecting the momentum dependence of its EPC. Among them mode-mode coupling and induced critical fluctuations [12,13], as well as anharmonicity in the soft mode phonon dispersion of $2H\text{-NbSe}_2$ [41,42] have been proposed. Note that in that respect our hybridization model is a special case of mode-mode coupling theories.

III. CONCLUDING REMARKS

In conclusion, we have presented a simple and general explanation of the thermal dependence of the modulation wave

vector observed in different classes of CDW systems. This variation relies on the thermal dependence of the electron-hole coherence length which fixes the rigidity of the CDW sublattice with respect to a variation of its modulation wave vector. This calculation allowed us to quantitatively obtain the momentum variation of the EPC of $\text{K}_{0.3}\text{MoO}_3$ and to explain its variation by the hybridization of a critical polar optical branch, strongly coupled to the 1D electron gas, with a less coupled acoustic branch. Finally, as similar $\delta q(T)$ variations are observed in SDW materials such as Cr [43] and GdSi [44], we suggest that Eq. (8) could also explain the thermal dependence of the SDW modulation on the basis of a q dependent coupling $\lambda(q) = 2U(q) - V(q)$ involving nonlocal Coulomb/exchange interactions [25].

ACKNOWLEDGMENTS

This work was supported by Spanish MICIU through Grant No. PGC2018-096955-B-C44 and the Severo Ochoa FUNFUTURE (CEX2019-000917-S) Excellence Centre distinction, and Generalitat de Catalunya (Grant No. 2017SGR1506).

-
- [1] D. I. Khomskii, *Basic Aspects of the Quantum Theory of Solids: Order and Elementary Excitations* (Cambridge University Press, Cambridge, 2010).
- [2] E. Fradkin, S. A. Kivelson, and J. M. Tranquada, *Rev. Mod. Phys.* **87**, 457 (2015).
- [3] K. Rossnagel, *J. Phys.: Condens. Matter* **23**, 213001 (2011).
- [4] T. Ishiguro, K. Yamaji, and G. Saito, *Organic Superconductors*, 2nd ed. (Springer, Berlin, 1998).
- [5] M. J. Rice and S. Strässler, *Solid State Commun.* **13**, 125 (1973).
- [6] J.-P. Pouget, *C. R. Phys.* **17**, 332 (2016).
- [7] B. Guster, M. Pruneda, P. Ordejón, E. Canadell, and J.-P. Pouget, *Phys. Rev. Materials* **3**, 055001 (2019).
- [8] B. Guster, M. Pruneda, P. Ordejón, E. Canadell, and J.-P. Pouget, [arXiv:2012.06812v2](https://arxiv.org/abs/2012.06812v2) [cond-mat.mtrl.sci].
- [9] M. D. Johannes and I. I. Mazin, *Phys. Rev. B* **77**, 165135 (2008).
- [10] $g(k, q)$ quantifies the scattering of a $|k\rangle$ state electron to a $|k+q\rangle$ electronic state with the absorption of a phonon of momentum q .
- [11] S. Barisic, J. Labbé, and J. Friedel, *Phys. Rev. Lett.* **25**, 919 (1970).
- [12] F. Flicker and J. van Wezel, *Nat. Commun.* **6**, 7034 (2015).
- [13] F. Flicker and J. van Wezel, *Phys. Rev. B* **94**, 235135 (2016).
- [14] J. Henke, F. Flicker, J. Laverock and J. van Wezel, *SciPost Phys.* **9**, 056 (2020).
- [15] J. Berges, E. G. C. P. van Loon, A. Schobert, M. Rösner, and T. O. Wehling, *Phys. Rev. B* **101**, 155107 (2020).
- [16] F. Weber, S. Rosenkranz, J.-P. Castellán, R. Osborn, R. Hott, R. Heid, K.-P. Bohnen, T. Egami, A. H. Said, and D. Reznik, *Phys. Rev. Lett.* **107**, 107403 (2011).
- [17] M. Maschek, S. Rosenkranz, R. Heid, A. H. Said, P. Giraldo-Gallo, I. R. Fischer, and F. Weber, *Phys. Rev. B* **91**, 235146 (2015).
- [18] X. T. Zhu, Y. W. Cao, J. D. Zhang, E. W. Plummer, and J. D. Guo, *Proc. Natl. Acad. Sci. USA* **112**, 2367 (2015).
- [19] J. P. Pouget, C. Noguera, A. H. Moudden, and R. Moret, *J. Phys.* **46**, 1731 (1985).
- [20] H. G. Smith and G. H. Lander, *Phys. Rev. B* **30**, 5407 (1984).
- [21] W. L. McMillan, *Phys. Rev. B* **14**, 1496 (1976).
- [22] S. Ravy, S. Rouzière, J.-P. Pouget, S. Brazovskii, J. Marcus, J.-F. Bérar, and E. Elkaim, *Phys. Rev. B* **74**, 174102 (2006).
- [23] Y. Feng, J. van Wezel, J. Wang, F. Flicker, D. M. Silevitch, P. B. Littelwood, and T. F. Rosenbaum, *Nat. Phys.* **11**, 865 (2015).
- [24] C. M. Varma and W. Weber, *Phys. Rev. B* **19**, 4325 (1979).
- [25] S.-K. Chan and V. Heine, *J. Phys. F: Met. Phys.* **3**, 795 (1973).
- [26] A. H. Moudden, J. D. Axe, P. Monceau, and F. Levy, *Phys. Rev. Lett.* **65**, 223 (1990).
- [27] D. E. Moncton, J. D. Axe, and F. J. DiSalvo, *Phys. Rev. B* **16**, 801 (1977).
- [28] N. Ru, C. L. Condon, G. Y. Margulis, K. Y. Shin, J. Laverock, S. B. Dugdale, M. F. Toney, and I. R. Fisher, *Phys. Rev. B* **77**, 035114 (2008).
- [29] C. M. Varma and W. Weber, *Phys. Rev. Lett.* **39**, 1094 (1977).
- [30] The decoupling in Eq. (4) can be justified for the electronic structure of quasi-1D systems where the electronic velocity $|v_k| \approx v_F$ entering in the expression of the EPC given in Ref. [29] varies weakly with k .
- [31] C. Noguera and J.-P. Pouget, *J. Phys. I France* **1**, 1035 (1991).
- [32] M. D. Johannes, I. I. Mazin, and C. A. Howells, *Phys. Rev. B* **73**, 205102 (2006).
- [33] With the definition of the free energy given by Eq. (13), $\xi_{\text{ch}}^{\text{SC}}(T)$ given by Eq. (14) is $(T/\Delta)\xi_0$ of Ref. [31].
- [34] S. Girault, A. H. Moudden, and J. P. Pouget, *Phys. Rev. B* **39**, 4430 (1989).
- [35] J. P. Pouget, B. Hennion, C. Escribe-Filippini, and M. Sato, *Phys. Rev. B* **43**, 8421 (1991).
- [36] E. Tutiš and S. Barišić, *Phys. Rev. B* **43**, 8431 (1991).
- [37] M. Maschek, D. A. Zocco, S. Rosenkranz, R. Heid, A. H. Said, A. Alatas, P. Walmsley, I. R. Fisher, and F. Weber, *Phys. Rev. B* **98**, 094304 (2018).

- [38] B. M. Murphy, H. Requardt, J. Stettner, J. Serrano, M. Krisch, M. Müller, and W. Press, *Phys. Rev. Lett.* **95**, 256104 (2005).
- [39] S. Motizuki and E. Ando, *J. Phys. Soc. Jpn.* **52**, 2849 (1983).
- [40] S. Motizuki, K. Kimura, E. Ando, and N. Suzuki, *J. Phys. Soc. Jpn.* **53**, 1078 (1984).
- [41] M. Leroux, I. Errea, M. Le Tacon, S.-M. Souliou, G. Garbarino, L. Cario, A. Bosak, F. Mauri, M. Calandra, and P. Rodière, *Phys. Rev. B* **92**, 140303(R) (2015).
- [42] R. Bianco, L. Monacelli, M. Calandra, F. Mauri, and I. Errea, *Phys. Rev. Lett.* **125**, 106101 (2020).
- [43] S. A. Werner, A. Arrott, and H. Kendrick, *Phys. Rev.* **155**, 528 (1967).
- [44] Y. Feng, J. Wang, A. Palmer, J. A. Aguiar, B. Mihaila, J.-Q. Yan, P. B. Littlewood, and T. F. Rosenbaum, *Nat. Commun.* **5**, 4218 (2014).